# Efficient Technique for the Analysis of Electromagnetic Problems Involving Antenna Trajectories in Complex Scenarios

Carlos Delgado, Eliseo García, Lorena Lozano, and Manuel Felipe Cátedra, *Fellow, IEEE*

***Abstract*—This letter presents an efficient approach for the electromagnetic analysis of complex scenarios involving transmitting antennas moving along predetermined trajectories. In order to efficiently reduce the size of the problem for each position of the antenna, we propose a technique based on macro basis functions that are dynamically generated using a ray-tracing analysis. The multilevel fast multipole algorithm is also included in order to reduce the memory consumption and speed up the solution process. Some representative test cases serve to validate the efficiency and performance of the proposed approach.**

***Index Terms*—Electromagnetic analysis, macro basis functions (MBFs), numerical analysis, ray tracing.**

## I. Introduction

THERE is, nowadays, a wide variety of numerical approaches for the simulation of complex electromagnetic problems, covering a range of applications with different computational requirements. Although some of these techniques are included in commercial computer tools, there is an ongoing effort towards the development of more efficient variations of existing approaches.

The application of modern full-wave analysis methods in particular allows to address, in some cases, scenarios that were restricted in the past to high-frequency techniques [1]–[3], more relaxed regarding computational requirements. Taking the conventional method of moments (MoM) [4] as the boundary-element technique that constitutes the reference generally considered for the development of modern approaches, it is possible to identify some major groups of methods with respect to the nature of the strategy used for the efficiency improvement given as follows:

1) the storage of exclusively the near-field part of the coupling matrix, considering the far-field interactions via the computation of fast matrix–vector products in the solution process;
2) the reduction of the number of unknowns obtained by defining basis functions over extended domains, usually known as macro basis functions (MBFs) [5]–[7];
3) the use of domain-decomposition approaches, which allow to analyze separately different parts of the scenario and exchange data between the domains afterwards in order to obtain the final current distribution [8], [9].

It is possible, in many cases, to combine the methods belonging to the previously mentioned groups to obtain further improvements. For example, the multilevel fast multipole algorithm [10] is a popular efficient approach that allows fast matrix–vector products by aggregating the field radiated by clusters of currents to certain reference points, which are then combined with other multipoles, translated, and disaggregated in order to account for the interaction between distant parts of the geometry, and has been successfully combined with MBF-based methods [11] as well as with domain-decomposition techniques [8], [12]. The adaptive cross approximation [13] is an alternative to the multilevel fast multipole algorithm (MLFMA) that allows to compress coupling submatrices between distant parts of the scenario and has been combined with an MBF approach in [14].

Efficient methods are especially important in applications that require the full-wave analysis of multiple excitations separately, involving time-consuming simulations. The work presented here can be included under this context. More specifically, we present a numerical approach for the full-wave analysis of the radiation characteristics of transmitting antennas that move along predetermined trajectories on complex scenarios. This contribution can be applied to the study of the antenna placement on vehicular platforms such as satellites, aircrafts, ships, cars, etc., coverage optimization for indoor and outdoor mobile communications, or applications related to radar systems, and makes use of a strategy based on dynamically chosen MBFs for each point of the trajectory using ray-tracing data, as well as its combination with the MLFMA for improved efficiency. The presented approach can be used to analyze problems where conventional full-wave techniques are burdened by the computational requirements, allowing better accuracy than that offered by ray-tracing-based asymptotic methods and enabling the analysis of geometrical structures that fall out of their scope such as discontinuities, slits, surfaces containing periodical structures, or electrically small patches.

The ray-tracing computation is normally used with high-frequency techniques to obtain the propagation paths of the rays

Manuscript received December 20, 2019; revised January 23, 2020; accepted January 25, 2020. Date of publication January 28, 2020; date of current version March 3, 2020. This work was supported in part by the Spanish Ministry of Economy and Competitiveness under Project TEC2017-89456-R, in part by the Junta de Comunidades de Castilla-La Mancha under Project SBPLY/17/180501/000433, and in part by the University of Alcalá under Project CCG2018/EXP-048. *(Corresponding author: Carlos Delgado.)*

C. Delgado, L. Lozano, and M. F. Cátedra are with the Department of Computer Science, University of Alcalá, 28801 Madrid, Spain (e-mail: carlos.delgado@uah.es; lorena.lozano@uah.es; felipe.catedra@uah.es).

E. García is with the Department of Automatics, University of Alcalá, 28801 Madrid, Spain (e-mail: eliseo.garcia@uah.es).

Digital Object Identifier 10.1109/LAWP.2020.2969989

corresponding to different effects. It is not common to combine it with full-wave approaches, although the authors have made use of this analysis in the past in order to speed up existing approaches [12], [15], [16].

Section II describes the technique developed to address the problem described previously. Some representative results are shown in Section III with the purpose of assessing the performance and efficiency of the proposed method. A final discussion of the results obtained in this letter is presented in Section IV.

## II. Description of the Analysis Technique

Numerical techniques based on MBFs make use, on one hand, of the same kind of low-level basis functions used by the conventional MoM, such as Rao–Wilton–Glisson [6] functions or rooftops [11] and, on the other hand, of new sets of high-level basis functions (i.e., MBFs) that extend over cubical domains called blocks, with a typical side length of one or more wavelengths. The MBFs are aggregations of low-level basis functions inside a block with specific weights. The approach presented in this letter requires the computation of a number of *primitive* MBFs over each block and the reduced matrix containing the coupling terms between them. Using the ray tracing for each position of the antenna along the trajectory, a subset of the primitive MBFs is chosen and the rest discarded dynamically, allowing to speed up the analysis due to the reduction of the total number of unknowns.

MBF-based approaches require a compartmentalization of the geometry into a number of blocks that will be denoted $N_b$ in this letter. The term $B_k$ will make reference to the *k*th block of this partition. The application of this approach starts with the computation of the MBFs. For this purpose, each block is isolated from the rest of the geometry, and the currents induced by a number of samples of the plane wave spectrum (PWS) impinging on the block are calculated and subsequently arranged in the $[J]^i_{\mathrm{PWS}}$ matrix. The singular value decomposition (SVD) of this matrix produces a set of orthonormal singular vectors that serve as the primitive MBFs. The number of singular vectors to retain is determined using the corresponding singular values and a truncating threshold $T_{\max}$. The SVD of $[J]^i_{\mathrm{PWS}}$ can be expressed as

$$[J]^i_{\mathrm{PWS}} = [U] \begin{pmatrix} \sigma_1 & \dots & 0 & \\ \vdots & \ddots & \vdots & \ddots \\ 0 & \dots & \sigma_P & \end{pmatrix} [V]^* \tag{1}$$

where $\sigma_j$ is the *j*th singular value. Note that, for the application of the presented approach, in addition to the primitive MBFs, the singular values for each block are required to be stored. Assuming that these values are ordered and $\sigma_1$ represents that with a larger magnitude, the number of primitive MBFs for the *i*th block can be truncated, producing a reduced number of unknowns. The *j*th column of $[V]^*$ is to be selected as a new primitive MBF provided that the following criterion is satisfied:

$$\frac{\sigma_1}{\sigma_j} \leq T_{\max} \tag{2}$$

where $T_{\max}$ is the threshold with typical values of around $10^3$. Considering the high-level basis functions described previously, it is possible to write the matrix equation as

$$[Z_R][J] = [V] \tag{3}$$

where the reduced coupling matrix $[Z_R]$ contains the reaction terms between the MBFs.

Considering that the total number of MBFs is $M$ and the trajectory under analysis contains $Np$ locations of a transmitting antenna on a given scenario, (3) needs to be solved $N_p$ times using different excitations in order to obtain the induced currents for each position

$$[Z_R]_{M\times M}[J^{(i)}]_{M\times 1} = [V^{(i)}]_{M\times 1}, \quad \text{for i} = 1,\ldots,N_p \tag{4}$$

where the current and excitation vectors $[J^{(i)}]$ and $[V^{(i)}]$ are those associated to the *i*th position of the active antenna along the trajectory.

The solution of (3) or (4) is the coefficient vector of a linear combination of MBFs that approximates the original MoM solution. A higher singular value threshold $T_{\max}$ in (2) leads to more MBFs and better approximation, while a lower threshold leads to less MBFs and larger error.

The main idea presented in this letter is to adapt the threshold adaptively for each block depending on the expected contribution of that block to overall scattering. That is, if we expect a smaller relative contribution of block-i, we relax the approximation accuracy for that block by decreasing the singular value threshold to $T^{(i)} < T\max$. If done properly, this will result in a reduction of the total number of MBFs without significant loss of overall accuracy

$$[Z_R^{(i)}]_{M_i\times M_i}[\tilde{J}^{(i)}]_{M_i\times 1} = [\tilde{V}^{(i)}]_{M_i\times 1}, \quad \text{for i} = 1,\ldots,N_p \tag{5}$$

where $M_i$ is the reduced number of MBFs for the *i*th position of the antenna trajectory, $[Z_R^{(i)}]$ is the modified reduced coupling matrix, and $[\tilde{J}^{(i)}]$ and $[\tilde{V}^{(i)}]$ are, respectively, the versions of $[J^{(i)}]$ and $[V^{(i)}]$ that only retain the coefficients associated to the MBFs that have been selected. Note that $[Z_R^{(i)}]$ can be obtained by simply discarding information of the original $[Z_R]$ as determined by the data returned by the ray-tracing analysis of each scenario following the procedure detailed below.

Clearly, the highest relative contribution to overall antenna coupling comes from blocks that are close to the transmitting or the receiving antennas. However, according to the high-frequency theory, in electrically large complex scenarios there are other sources of wave scattering and field hot spots apart from the antenna location points (due to scattering phenomena like multiple reflections, transmission, diffraction, creeping waves, or any combination of them), which we call critical points. Blocks close to these critical points will also have a significant contribution to the overall computation. Thus, our criterion to adapt the singular value threshold $T^{(i)}$ will depend on the distance to the closest critical point

$$D_i = \min_{j=1,\ldots,N_c} (\|\vec{r}_b^{(i)} - \vec{r}_c^{(j)}\|) \tag{6}$$

where $\vec{r}_b^{(i)}$ indicates the position vector of the center of the *i*th block and $\vec{r}_c^{(j)}$ stands for the position vector of the *j*th critical point. We denote $D_i$ as the *critical distance* associated to the *i*th block. Fig. 1 displays an illustrative 2-D example of a scenario where the ray-tracing analysis for a position of the transmitting antenna has produced three rays (double transmission, diffraction, and double reflection), showing the location of

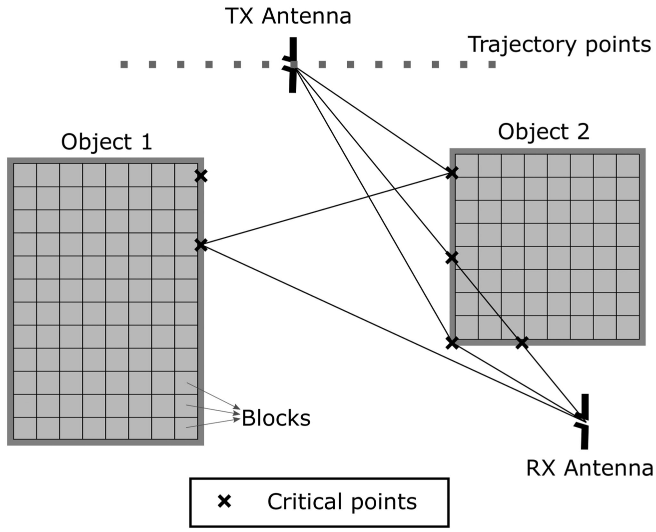


Fig. 1. Scheme illustrating the extraction of the critical points from the ray-tracing analysis in a 2-D scenario.

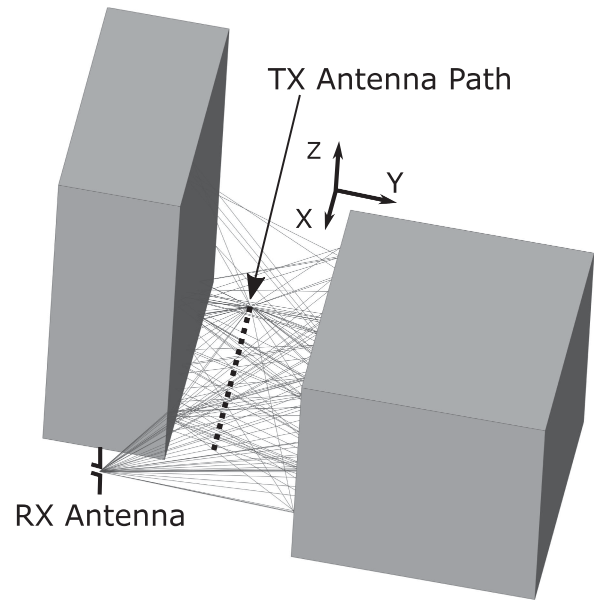


Fig. 2. Geometry of the first test case and ray-tracing analysis for the first trajectory point.

the corresponding critical points. Critical points are identified by the ray-tracing analysis of the scenario for a given position of the TX and RX antennas.

The critical distance is used to compute the threshold $T^{(i)}$ with which the MBFs are determined for the *i*th block, as indicated in [16]

$$T^{(i)} = \begin{cases} T_{\min} + \frac{\Delta_b^2 (T_{\max} - T_{\min})}{4D_i^2}, & \text{if } D_i \geq \frac{\Delta_b}{2} \\ T_{\max}, & \text{if } D_i < \frac{\Delta_b}{2} \text{ or } B_i \text{ contains caustics} \end{cases} \tag{7}$$

where $T_{\min}$ is the minimum threshold value allowed. While $T_{\max}$ corresponds to the fixed threshold used in conventional MBF approaches, the role of $T_{\min}$ is important to ensure that the current distribution on the scenario is continuous, even if the contribution of the block is not relevant. The block size is represented by $\Delta_b$. Note that (7) assigns the threshold value following an inverse square function of the critical distance for each block. The maximum threshold is applied when the nearest critical point is inside the block.

The new thresholds assigned to each block are used at this point to identify the primitive MBFs, to be retained or to be discarded for each particular analysis. Analogously to (2), the *j*th primitive MBF is to be selected provided that

$$\frac{\sigma_1}{\sigma_j} \leq T^{(i)} \tag{8}$$

and, after repeating the described procedure for each block and trajectory point, (5) can be solved in order to obtain the current distribution for each antenna position.

## III. Numerical Results

This section contains some simulations performed in order to validate the computational advantages that, from a theoretical point of view, can be derived from the description of the presented approach. The hardware platform used has been a Supermicro 2027GR-TRF server containing two Intel Xeon E5-2690 2.9 GHz processors with a total of 16 physical cores and 256 GB of RAM. The iterative solver has been BiCGStab(l) [17] with a maximum residual of $10^{-3}$ and using the sparse approximate inverse preconditioner described in [18]. All the coordinates used in this section for the description of point locations are expressed in meters.

The first test case considered is described by two perfect electric conductor (PEC) boxes. One of them is a cube centered at (2.5, 2.5, 2.5) with a side length of 5 m. The second box is centered at (0.5, −4.25, 3.75), and its dimensions along *X*, *Y*, and *Z* are, respectively, 5, 2.5, and 7.5 m. The transmitting antenna moves along a path from a starting point at (−2, −2, 1) and a final point at (1, −2, 1), considering 31 intermediate sampling positions that define the same number of problems. The coupling between the transmitting antenna and a receiving antenna located at (5, −4, 1.5) has been analyzed. This scenario is shown in Fig. 2, including the visualization of the ray-tracing results for the first point of the trajectory path of the transmitting antenna.

This case has been simulated considering the combined field integral equation (CFIE) formulation at a frequency of 1 GHz using the MoM-MLFMA approach as well as the conventional characteristic basis function method (CBFM)-MLFMA and the technique proposed in this letter. The total number of low-level unknowns has been 649 152. By applying the CBFM-MLFMA technique, the size of the problem has been reduced to 173 931 MBFs using a block size of λ. The proposed approach, in turn, has made use of an average of 80 715 MBFs. The average number of rays and critical points on the scenario has been 34 and 115, respectively. The CPU-times required for the simulation of this test case are shown in Table I. The setup stage includes the time required to compute the near-field coupling terms as well as the multipole data and, in the case of MBF-derived approaches, the generation of the high-level basis functions. Fig. 3 plots the results returned by the simulations. We can conclude from these results that the proposed approach presents good accuracy and efficiency for this test case.

TABLE I
CPU-TIME REQUIRED FOR THE FIRST TEST CASE

| Approach | Setup Stage | Solution Stage |
|---|---|---|
| **MoM-MLFMA** | 552 s | 5,875 s |
| **MBF-MLFMA** | 2,177 s | 2,945 s |
| **Proposed Technique** | 2,177 s | 1,677 s |

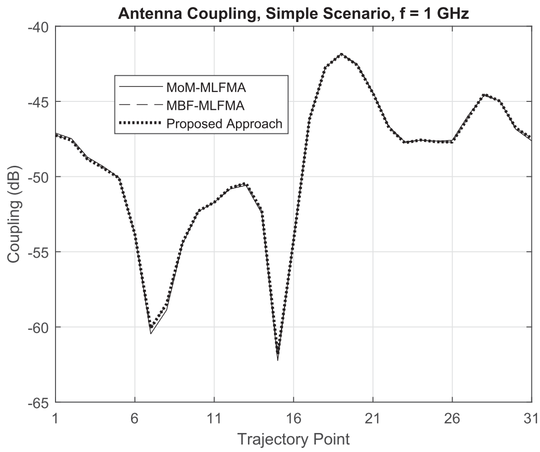


Fig. 3. Antenna coupling results for the first test case.

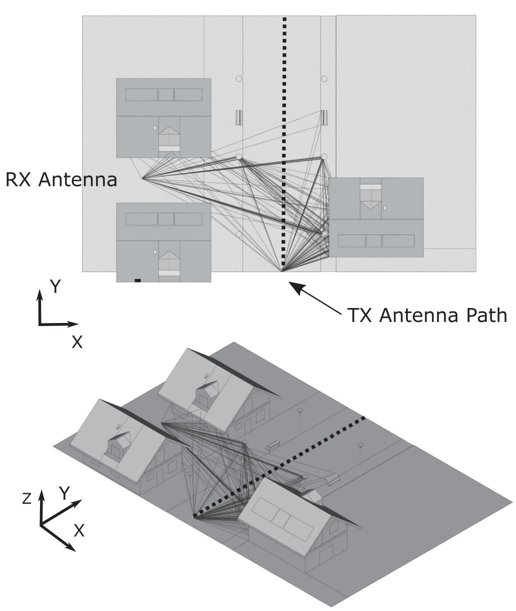


Fig. 4. Geometry of the second test case, including top view (top) and axonometric view (bottom) and ray-tracing analysis for the first trajectory point.

The next example contains a small suburban landscape modeled using 454 nonuniform rational B-spline surfaces, including three houses, two seats, six street lamps and the corresponding gardens, sidewalks, and a main road. For the sake of simplicity, this problem has been analyzed considering PEC surfaces. The size of the scenario is approximately 50 m long and 33 m wide. The coupling between a dipole antenna moving along the main road and a passive antenna located between two houses has been obtained at 850 MHz, considering 33 positions for the active antenna separated by 1 m. Fig. 4 illustrates the geometry involved in this test case, including the ray-tracing data for the first point.

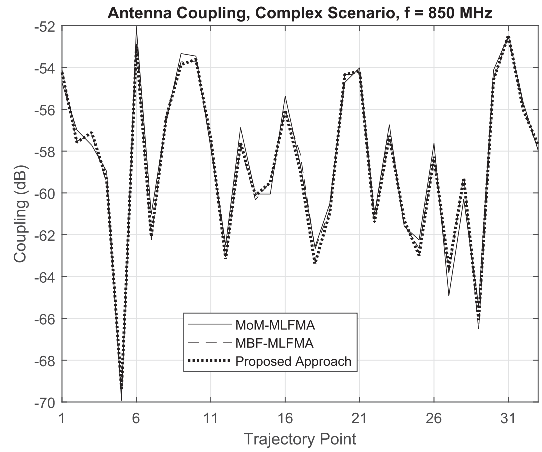


Fig. 5. Antenna coupling results for the second test case.

TABLE II
CPU-TIME REQUIRED FOR THE SECOND TEST CASE

| Approach | Setup Stage | Solution Stage |
|---|---|---|
| **MoM-MLFMA** | 2,699 s | 311,520 s |
| **MBF-MLFMA** | 7,531 s | 108,240 s |
| **Proposed Technique** | 7,531 s | 53,414 s |

As in the previous example, the CFIE formulation has been used to compute the results using MoM-MLFMA, CBFM-MLFMA, and the proposed approach. The MoM-MLFMA approach required the solution of a problem containing 3 155 750 unknowns. Using blocks with a size of $\lambda$ as in the previous example, the number of unknowns has been reduced with the CBFM-MLFMA technique to 1 320 390. Using the proposed approach, we observe a noteworthy reduction down to an average of 684 540 high-level unknowns. Fig. 5 plots the coupling results returned by the three methods, showing a good agreement between them. The average numbers of rays and critical points for the positions of the trajectory have been 155 and 423, respectively. Table II shows the time required by the techniques considered to reach the solution, serving as a validation of the efficiency of the presented approach.

## IV. CONCLUSION

An efficient technique for the full-wave electromagnetic analysis of variable antenna positions on complex scenarios has been presented in this work. This approach makes use of a ray-tracing-based modification of conventional MBF methods in order to minimize the number of high-level unknowns for each antenna location, as well as the combination with the multilevel fast multipole algorithm for a faster computation of the matrix–vector products required by the solution process and a lesser memory footprint of the coupling matrix. Some representative examples show good accuracy and improved performance over conventional MoM-MLFMA or MBF approaches.

## REFERENCES


[1] E. F. Knott, "A progression of high-frequency RCS prediction techniques," *Proc. IEEE*, vol. 73, no. 2, pp. 252–264, Feb. 1985.

[2] M. F. Cátedra, C. Delgado, S. Luceri, and F. Sáez de Adana, "Efficient procedure for computing fields created by current modes," *Electron. Lett.*, vol. 39, pp. 763–764, May 2003.

[3] M. F. Cátedra, C. Delgado, S. Luceri, O. González, and F. Sáez de Adana, "Physical optics analysis of multiple interactions in large scatters using current modes," *IEEE Trans. Antennas Propag.*, vol. 54, no. 3, pp. 985–994, Mar. 2006.

[4] R. F. Harrington, *Field Computation by Moment Methods*. New York, NY, USA: Macmillan, 1968.

[5] E. Suter and J. R. Mosig, "A subdomain multilevel approach for the efficient MoM analysis of large planar antennas," *Microw. Opt. Technol. Lett.*, vol. 26, no. 4, pp. 270–277, Aug. 2000.

[6] V. V. S. Prakash and R. Mittra, "Characteristic basis function method: A new technique for efficient solution of method of moments matrix equation," *Microw. Opt. Technol. Lett.*, vol. 36, no. 2, pp. 95–100, Jan. 2003.

[7] C. Delgado, R. Mittra, and M. F. Cátedra, "Accurate representation of the edge behavior of current when using PO-derived characteristic basis functions," *IEEE Antennas Wireless Propag. Lett.*, vol. 7, no. 5, pp. 43–45, Mar. 2008.

[8] I. Gonzalez, A. Tayebi, J. Gomez, C. Delgado, and M. F. Cátedra, "Fast analysis of a dual-band reflectarray using two different numerical approaches based on the moment method," *IEEE Trans. Antennas Propag.*, vol. 61, no. 4, pp. 2333–2336, Apr. 2013.

[9] K. Zhao, V. Rawat, and J.-F. Lee, "A domain decomposition method for electromagnetic radiation and scattering analysis of multi-target problems," *IEEE Trans. Antennas Propag.*, vol. 56, no. 8, pp. 2211–2221, Aug. 2008.

[10] W. C. Chew, J. Jin, E. Michielssen, and J. Song, Eds., *Fast and Efficient Algorithms in Computational Electromagnetics*. Norwood, MA, USA: Artech House, 2001.

[11] E. Garcia, C. Delgado, I. González, and M. F. Cátedra, "An iterative solution for electrically large problems combining the characteristic basis function method and the multilevel fast multipole algorithm," *IEEE Trans. Antennas Propag.*, vol. 56, no. 8, pp. 2363–2371, Aug. 2008.

[12] C. Delgado, E. García, and M. F. Cátedra, "Ray-tracing based dual domain analysis technique using the method of moments and the multilevel fast multipole algorithm," *IEEE Trans. Antennas Propag.*, vol. 67, no. 12, pp. 7496–7504, Dec. 2019.

[13] J. M. Tamayo, A. Heldring, and J. M. Rius, "Multilevel adaptive cross approximation (MLACA)," *IEEE Trans. Antennas Propag.*, vol. 59, no. 12, pp. 4600–4608, Dec. 2011.

[14] X. Chen, C. Gu, J. Ding, Z. Li, and Z. Niu, "Multilevel fast adaptive cross-approximation with characteristic basis functions," *IEEE Trans. Antennas Propag.*, vol. 63, no. 9, pp. 3994–4002, Sep. 2015.

[15] C. Delgado and M. F. Cátedra, "Combination of ray-tracing and the method of moments for electromagnetic radiation analysis using reduced meshes," *J. Comput. Phys.*, vol. 361, pp. 412–423, May 2018.

[16] C. Delgado and M. F. Cátedra, "Efficient generation of macro basis functions for radiation problems using ray-tracing derived dynamic thresholds," *IEEE Trans. Antennas Propag.*, vol. 66, no. 6, pp. 3231–3236, Jun. 2018.

[17] G. L. G. Sleijpen and D. R. Fokkema, "Bi-CGSTAB(l) for linear equations involving unsymmetric matrices with complex spectrum," *Electron. Trans. Numer. Anal.*, vol. 1, pp. 11–32, 1993.

[18] C. Delgado and M. F. Cátedra, "Sparse approximate inverse preconditioner with parametric sparsity pattern applied to macro basis function methods," *IEEE Antennas Wireless Propag. Lett.*, vol. 17, no. 5, pp. 849–852, May 2018.